

***Ab-Initio* Calculations of Photonic Structures**

Academic and Research Staff

Professor J. D. Joannopoulos
Professor Marin Soljačić

Visiting Scientists and Research Affiliates

Dr. Bjorn Maes

Postdoctoral Fellows

Dr. Mihai Ibanescu
Dr. Jorge Bravo-Abad
Dr. Peter Bermel
Dr. Peter Rakich
Dr. Zheng Wang

Graduate Students

Aristeidis Karalis
David Chan
Michael Ghebrebrhan
Rafif Hamam
Yidong Chong
Andre Kurs
Alejandro Rodriguez

Undergraduate Students

Robert Moffatt
Manisha Padi

Technical and Support Staff

Margaret O'Meara

Summary

We propose an on-chip optical waveguide for Bose-Einstein condensates based on the evanescent light fields created by surface states of a photonic crystal. It is shown that the modal properties of these surface states can be tailored to confine the condensate at distances from the chip surface significantly longer than those that can be reached by using conventional index-contrast guidance. We numerically demonstrate that by index-guiding the surface states through two parallel waveguides, the atomic cloud can be confined in a two-dimensional trap at about $1\mu\text{m}$ above the structure using a power of 0.1mW .

Photonic crystal optical waveguides for on-chip Bose-Einstein condensates

Project Staff

Jorge Bravo-Abad
Mihai Ibanescu
J. D. Joannopoulos
M. Soljačić

One of the key ingredients for the development of an atom-chip technology based on the coherent manipulation of matter waves is the design of efficient atomic waveguides able to

connect the different elements of these atom chips. Microfabricated structures able to guide Bose-Einstein condensates (BECs) have been proposed as a promising way to implement on-chip matter-wave waveguides¹. In these experiments the BEC cloud is confined by means of magnetic field traps produced by currents flowing through microwires. However, the technology based on magnetic trapping is restricted by a fundamental limitation: the trapping mechanism works for only a subset of hyperfine states for any given trapping magnetic field. It has been shown that this limitation can be circumvented in a purely optical trap, where atoms in all hyperfine states can be confined². In fact, a large fraction of BEC experiments now use optical traps for these reasons. When working with an optical trap, one has the possibility of using an external magnetic field in order to access Feshbach resonances. In particular, the atomic interaction of a BEC in an optical trap can be modified by simply varying the external magnetic field, which eventually can lead to a BEC with nearly zero scattering length³. This could be of paramount importance for the development of efficient Sagnac interferometers based on the interference between two counterpropagating matter waves.

Due to the above mentioned interest, different kinds of dielectric structures have been proposed as optical traps⁴⁻¹³. One of these advances has been the experimental demonstration of the confinement of a BEC close to a dielectric surface by means of a gravito-optical surface trap (GOST)¹³. In a GOST scheme, the evanescent fields are produced by a blue-detuned laser beam undergoing total internal reflection (TIR) on the surface of a prism. The incidence angle from the high-index material into air has to be close to the critical angle for TIR, in order to make the evanescent field tails long. If this restriction is not satisfied, the strong short-range Casimir-Polder attraction cannot be balanced¹⁴. In this type of systems the horizontal confinement is obtained by means of a second red-detuned laser source that results in the appearance of a narrow potential well in the transverse plane. Therefore, the extension of this idea to create optical on-chip BEC waveguides and circuits is limited.

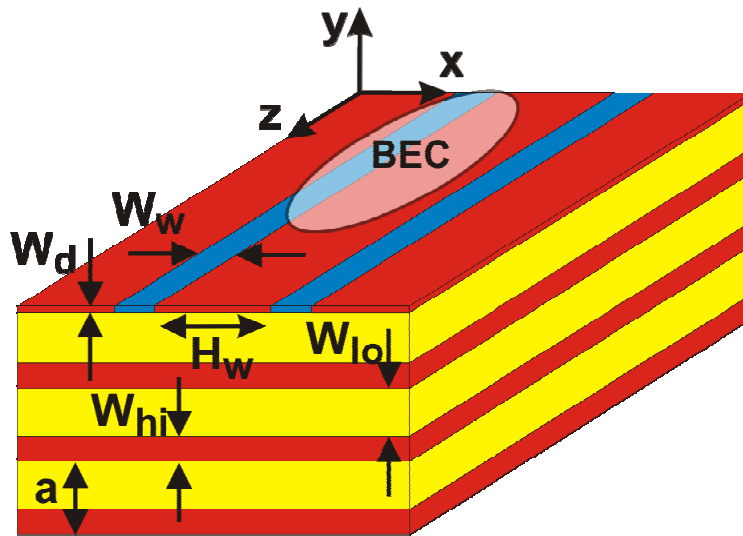


Figure 1: Schematic picture of the structure proposed for BEC waveguiding. The system consists of a one-dimensional photonic crystal with a defect layer on its top. In the defect layer two parallel index-guiding waveguides are included. As it is sketched in the figure, for a suitable design of the system, the BEC cloud can be confined in the region between these waveguides. The reference system used throughout the text, together with the geometrical parameters defining the structure are also shown.

The simplest scheme one could imagine for on-chip waveguiding of BECs would be to use evanescent tails of a mode of a high-index waveguide deposited on top of a uniform dielectric substrate of dielectric constant ϵ_{subs} . If we illuminate this waveguide, the corresponding electric field will be confined within it, provided that the dielectric constant of the substrate is smaller than that of the waveguide. In order to have index-guiding in the waveguide, without leakage into the substrate, the wave vector k of the guided mode has to satisfy: $k > (\omega/c)\sqrt{\epsilon_{subs}}$. This in turn means that the decay constant of the evanescent tails into air is given by $\alpha = \sqrt{k^2 - \omega^2/c^2} > (2\pi/\lambda_{AIR})\sqrt{\epsilon_{subs}-1}$, where λ_{AIR} is the wavelength of light in air. Because ϵ_{subs} cannot be close to unity (it is typically larger than 2.0), this is a fast decay that would prevent the above-mentioned balance between the repulsion from the surface and the Casimir-Polder attraction. For similar reasons, same constraints apply for any index-guided scheme that involves a solid-state substrate for which $\epsilon_{subs} \sim 1$. On the other hand, designs without a substrate would have thickness $< \lambda_{AIR}$, rendering them very fragile and difficult to work with. In this work, we move a step forward and we show that the use of a photonic crystal (PhC) as a substrate would permit to have decay lengths long enough to circumvent the limits imposed by the Casimir-Polder attraction.

Keeping in mind the previous considerations, we propose a novel GOST design for optical guiding of BECs. In our system the evanescent light fields are created by surface states of one-dimensional photonic crystals¹⁵ (1D-PhCs). Surface states are prohibited from propagating into the PhC bulk by photonic bandgap effects, and are prevented from leaking into air because of TIR effects; thus, they are confined to propagate along the surface. Surface states of this kind are unique to PhCs. Our system presents several advantages over other approaches suggested until now for purely optical BEC waveguiding. First of all, we will demonstrate that a suitably chosen surface state of a 1D-PhC can have the long electric-field evanescent tails needed in realistic designs of the basic elements for atomic circuits. Furthermore, we will show that the design we currently propose allows straightforward tuning of the atomic potential shape using only one laser source. Finally, it is worth noting that these are realistic designs, as they can be produced with the current microfabrication technology.

Figure 1 shows a schematic picture of the structure analyzed in this work for on-chip BEC waveguiding. The main idea proposed here to get a confining potential both in the x- and y-directions (see the reference system in Fig. 1) is the following. First, we create a 1D-PhC by a periodic sequence of a high dielectric constant (ϵ_{hi}) and a low dielectric constant (ϵ_{lo}) layers (plotted as red and yellow volumes in Fig. 1, respectively). The thickness of each layer is given by W_{hi} and W_{lo} . In addition, we define a as the periodicity of the PhC. Secondly, we introduce a defect in this structure by reducing the thickness of its top layer to W_d . The electric field of this defect mode is confined both in $y>0$ and $y<0$ regions, i.e., this mode is a surface state. By coupling into the defect layer a laser beam whose frequency is blue-detuned from a certain transition of the atoms forming the considered BEC, the condensate will experience a repulsive potential from the surface. This potential combined with the Casimir-Polder interaction and the force exerted by the gravity (which pushes the atoms towards the surface) will trap the BEC in the minimum of the potential in the y-direction.

Once a suitable confinement in the direction normal to the air-PhC interface is obtained, the next step is to design a practical mechanism to confine the BEC in the x direction. We have found that one convenient way to achieve this is to create two index-guided parallel waveguides for these surfaces states, (represented as blue volumes in Fig. 1, where W_w and H_w stand for the width of the waveguides and the separation between them, respectively). Intuitively, the atomic potential produced by these waveguides consists of two bumps in the x-direction with a minimum between them, in which the atomic cloud can be trapped. Notice that by changing H_w and/or the power carried by the electromagnetic mode of the two waveguides, we can also tune the curvature of the proposed two-dimensional potential well, allowing us to design the shape of the BEC to our convenience.

In order to optimize the potential created by the structure described in the previous paragraphs we first analyze the case in which the PhC is uniform in the x-direction (i.e. without waveguides). This is a good starting point because the decay of the electric field in the y-direction will be almost the same as in the system with the two waveguides¹⁶.

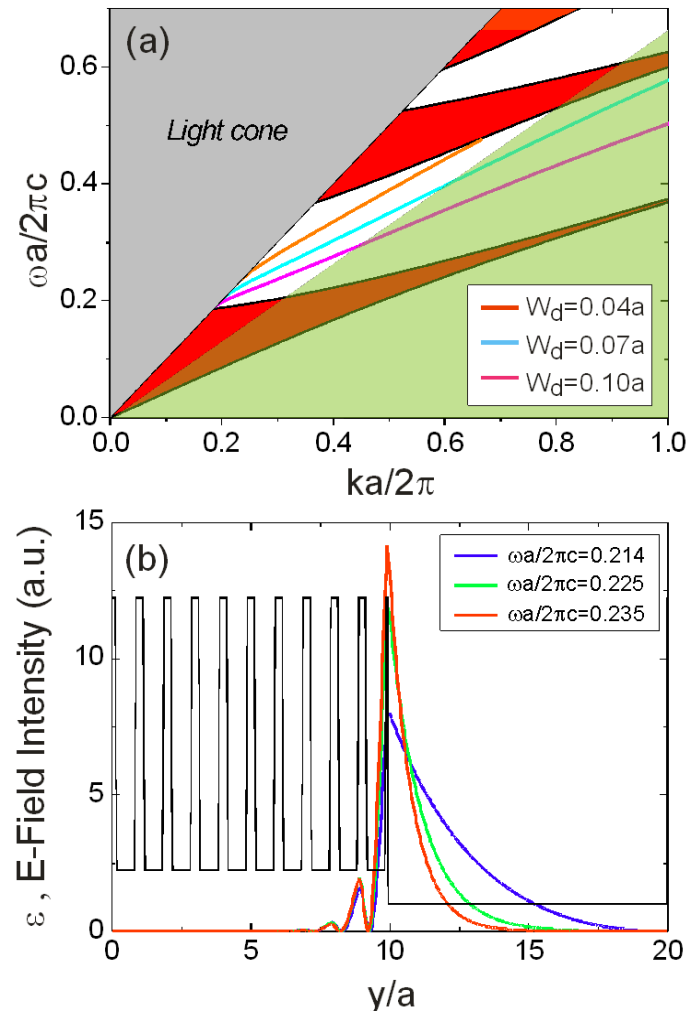


Figure 2: Properties of the surface states created by introducing a defect layer on top of the photonic crystal. (a) Projected band structure of the semi-infinite one-dimensional photonic crystal (PhC) considered in this work [see the profile of dielectric constant in panel (b)]. Red shaded areas show the regions where there exist extended states inside the PhC. Grey shaded area corresponds to eigenmodes that are propagating in air. Orange, blue and magenta lines represent the dispersion relations of the surface states for several values of the thickness of the top layer. Green shaded region corresponds to possible confined states of any defect layer if it lies on top of a uniform dielectric substrate with $\epsilon = \epsilon_0$. (b) Dielectric constant (black line) and electric field intensity profiles along the direction perpendicular to the interface PhC-air. Three surface states with frequencies close to the light line are displayed for $W_d=0.07a$. Notice the increase of the decay length of the electric field as the frequency becomes closer to the light line (i.e. frequency decreases) and the rapid decay of the three modes inside the PhC.

Red regions in Fig. 2(a) show the projected bands of a semi-infinite 1D-PhC computed by means of the plane-wave expansion method to Maxwell's equations¹⁷. We have taken the following values for the parameters defining the structure $\epsilon_{hi}=12.25$, $\epsilon_{lo}=2.25$ and $W_{lo}=0.7a$, as they are typical values that could be used in the experiments. In addition we have assumed $\epsilon=1$ in the region above the PhC. The grey shaded region represents modes that can propagate in air. In order to show how the dispersion relation for the surface state changes with the thickness of the defect layer, we have also plotted in Fig. 2(a) the results for three different values of W_d (magenta, blue and orange lines correspond to $W_d = 0.04a$, $W_d = 0.07a$ and $W_d = 0.1a$). Any of these values for W_d could be chosen for our design; for definiteness, from now on we take $W_d = 0.07a$.

Now, let's turn our attention to study how the electric field profile depends on the frequency of the defect mode. Figure 2(b) shows a cross-section in the y -direction of electric field intensities of the surface states corresponding to three representative frequencies near the light line. Blue, green and red lines render the results for $\omega a/2\pi c=0.214$, $\omega a/2\pi c=0.225$ and $\omega a/2\pi c=0.235$, respectively. The profile of the dielectric constant along the y -direction of the structure has also been plotted. As it is expected, the decay length in air increases as we get closer to the light line (i.e. as the frequency decreases). This tunability of the evanescent tails of the electric field, without changing the geometrical parameters of the structure, makes the surface states of PhC promising candidates for the design of optical trapping potentials for BECs.

At this point, it is worth taking a closer look at the advantages of the type of systems studied in this manuscript compared with other kinds of rigid dielectric structures that are not based on PhCs. As it is shown in Fig. 2(a), the dispersion relation of the defect mode of a PhC allows us to choose a frequency as close to the light line as we need in our atomic trap design; thereby, the decay length in air can be tuned to be arbitrarily long. However, this property could not be obtained by means of any TIR-based waveguide placed on top of a dielectric substrate, as in that case the frequencies of the confined states ω_d are such that $\omega_d < ck / \sqrt{\epsilon_s}$, where ϵ_s is the dielectric constant of the substrate. This point is illustrated in Fig. 2(a), where the green shaded area corresponds to the region where confined states can exist for the case $\epsilon_s=\epsilon_{lo}$. As we can see in that figure, all of those states are far from the light line, so their decay length in air is short.

Now, before proceeding with the analysis of the full waveguiding structure, let's examine the confining atomic potential created by the 1D-PhC with a defect described previously, but without waveguides. If we illuminate this defect layer with a laser beam whose frequency ω is blue-detuned with respect to a certain atomic transition of frequency ω_0 , then an atom located above the PhC will experience a potential given by the sum of the optical-dipole (U_{op}), gravitational (U_{gv}), and Casimir-Polder interactions (U_{CP}), that is,

$$U(\vec{r}) = U_{op}(\vec{r}) + U_{gv}(\vec{r}) + U_{CP}(\vec{r})$$

The optical dipole contribution can be written as^{14,18} (1)

$$U_{op}(\vec{r}) = \beta_s \frac{\hbar \Gamma^2}{8\Delta} \frac{I(\vec{r})}{I_{sat}} \quad (2)$$

where β_s , I_{sat} are two parameters whose value depend on the atomic transition we are considering, Γ is the corresponding linewidth and $\Delta = \omega - \omega_0$ (note that in deriving Eq.(1), it has

been assumed that $|\Delta| \ll \omega_0$). $I(\vec{r}) \equiv \frac{1}{2} \epsilon_0 |\vec{E}(\vec{r})|^2$ is the electric field intensity. Since we are currently assuming that our structure has translational symmetry both in the x and z directions, we can write $I(\vec{r}) = I_0 \exp(-2y/\Lambda)$, where Λ defines the evanescent decay length of the electric field and I_0 is the intensity just above the illuminated layer.

The second term in Eq.(1) represents the gravitational potential and its given by $U_{gv}(\vec{r}) = mgy$, where m and g stand for the mass of each atom and the gravitational acceleration, respectively. Finally, the last term of Eq.(1) corresponds to the so-called Casimir-Polder potential $U_{CP}(\vec{r}) = -C_4 / y^3$, where the constant C_4 is given by¹⁹

$$C_4 = \frac{3\hbar c \alpha}{32\pi^2 \epsilon_0} \psi(\epsilon_{hi}) \quad (3)$$

In the above expression, α is the atomic polarizability and the value $\psi(\epsilon_{hi} = 12.25) \approx 0.69$ has been computed using the analytical expressions for the function $\psi(\epsilon_{hi})$ given by Yan *et al.*^{20,21}

In order to show the feasibility of the experimental realization of the system presented in this work, we consider the case of Cs atoms, since the confinement of a condensate of Cs atoms in a similar structure has been demonstrated¹³. As we are considering the D₂ resonant transition, we must take the following values in Eq. (1), $\beta_s=2/3$, $I_{sat}=1.1$ mW/cm², $\omega_0=2\pi \times 3.5 \times 10^{14}$ Hz ($\lambda_0=857.1$ nm), and $\Gamma=2\pi \times 5.3 \times 10^6$ Hz. Regarding the external illumination, we assume that it is produced by a Ti:sapphire laser at $\omega=2\pi \times 3.6 \times 10^{14}$ Hz. In addition, to get an optical potential with a similar depth to that obtained in Ref. 15, we suppose that the maximum electric field intensity in the air region very close to the PhC-air interface is $I_0=2.67 \times 10^6$ mW/cm².

Figure 3 plots the total atomic potential as a function of the distance from the surface for several values of the decay length Λ ranging from 0.1 to 0.6 μ m. As it is shown in this figure, a decrease in Λ leads to a shift of the minimum of the potential towards the surface. However as can be seen, there exists a minimum distance from the surface where the condensate can be trapped, since if we take $\Lambda < 0.2 \mu$ m the total potential does not have a minimum. This limit is established by the fact that in the region where the repulsive optical potential is not negligible for $\Lambda < 0.2 \mu$ m, the Casimir-Polder attractive interaction dominates, preventing the formation of a minimum in the total potential. In the case of the corresponding TIR waveguide design with a substrate with $\epsilon_{subs} = 2.25$ one would obtain a maximum decay length $\Lambda < 0.12 \mu$ m; thus, given the rapid variation of Casimir-Polder interaction as a function of distance, this demonstrates explicitly that a TIR scheme can not be made to work for the current purpose, and that PhCs indeed have to be used.

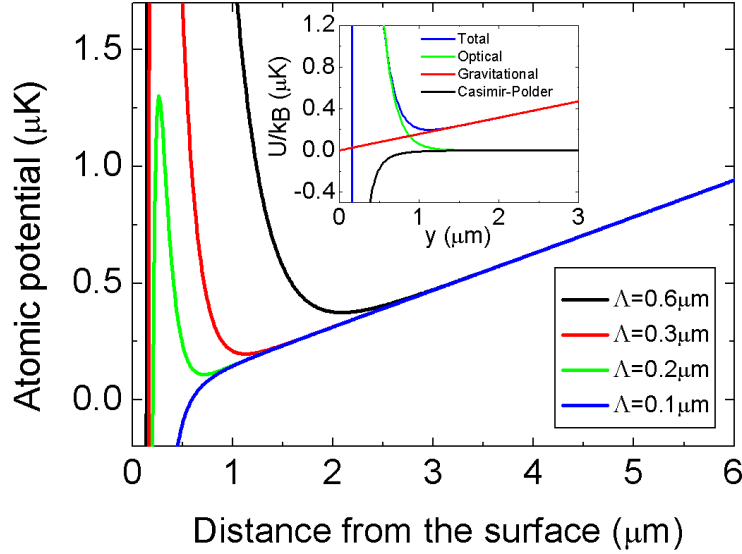


Figure 3: Atomic potential produced by illuminating the defect layer of the photonic crystal. Main panel: Total atomic potential for the case of Cs atoms as a function of the distance to the dielectric surface. The results for several decay lengths of the evanescent light field are shown. The optical dipole potential is assumed to be created by a Ti:sapphire laser at a wavelength of 839nm. All the cases plotted in this figure were computed for the same intensity $I_0=2.67 \times 10^6$ mW/cm² evaluated just above the PhC-air interface. Notice, how Casimir-Polder attractive potential prevents the creation of a BEC trap for $\Lambda < 0.2 \mu\text{m}$. Inset: Total, optical, gravitational and Casimir-Polder potentials (blue, green, red and black, respectively) for the case of $\Lambda = 0.3 \mu\text{m}$. The minimum for the total potential is found at $y_0 = 1.1 \mu\text{m}$.

Since we are interested in bringing the BEC as close as possible to the surface, we will choose $\Lambda=0.3\mu\text{m}$. This value corresponds to a state of wavevector $ka/2\pi=0.27$ of the defect band, and thereby a value of the periodicity $a=0.19\mu\text{m}$ (see Fig. 2(a)). From now on, we will assume this value of k , unless otherwise stated. In that case, the minimum of the potential appears at $y_0=1.1\mu\text{m}$.

It is also interesting to analyze the contribution of each term appearing in Eq.(1) to the total atomic potential. Blue, green, red, and black lines in the insert of Fig. 3 show the total, optical, gravitational and Casimir-Polder potentials, respectively, for $\Lambda=0.3\mu\text{m}$. This figure reveals that at small distances the Casimir-Polder potential governs the behavior of the total potential while for distances slightly larger than y_0 , the total potential is dominated by the gravitational interaction.

Finally, let us focus on how to obtain a suitable confining potential in the x-direction, needed to create an optical BEC waveguide. As we described above, we could solve this problem by including in the defect layer two index-guided waveguides of dielectric constant ϵ_w , with $\epsilon_w > \epsilon_{hi}$ (see schematics in Fig.1). For definiteness, we take $\epsilon_w=18$. Equivalently, bearing in mind a possible experimental implementation, one could choose a smaller value of ϵ_w and a larger local thickness $W_d(x)$ of the defect layer. The mode we explore is the even mode of this system of two coupled waveguides. In order to reproduce faithfully the features that could be found in the experiments, we have simulated the structure using the Finite-Difference Time-Domain (FDTD) method²². The results obtained with this method come from exact solutions of the 3D Maxwell equations, except for the numerical discretization.

As we described in the introduction, one of the main advantages of our proposal is that there are several parameters that can be changed to our convenience. Through the previous calculations,

we have fixed the values of the thickness of the defect layer W_d , as well as the wavevector k and the frequency ω considered. In addition, now for simplicity, we fix the width of the waveguides to $W_w=2a$. Therefore, the remaining parameters in our optimization process are the distance between the waveguides H_w and the power P_0 carried by the even mode they create. We now look for the values of (H_w, P_0) such as the curvature of the potential at its minimum is similar both in the x - and the y -directions. This condition would be useful if we want to guide a cylindrical-shape BEC along our waveguide. In addition, notice that we require a low value of P_0 in order to have an efficient guiding system.

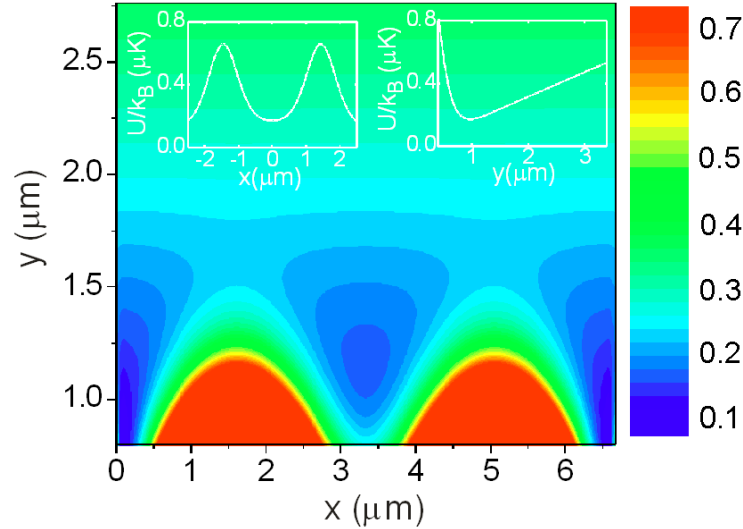


Figure 3: 2D total atomic potential produced by the structure sketched in Fig. 1 in the xy plane for the case of Cs atoms. Color scale codes the potential in units of μK . The minimum is found at $(x_0, y_0) = (3.3, 1.1)\mu\text{m}$. Left and right insets show cross-sections of the potential along the lines $y_0 = 1.1\mu\text{m}$ and $x_0 = 3.3\mu\text{m}$, respectively.

Following the program described above, we have found a suitable configuration for $H_w=3.2\mu\text{m}$ and $P_0=0.1\text{mW}$. Figure 4 shows a contour plot of the corresponding two dimensional total atomic potential in the xy plane. The color scale codes the potential in units of μK . This figure shows a minimum at $(x_0, y_0) = (3.3, 1.1)\mu\text{m}$, being the center of the waveguides located at $x_1=1.5\mu\text{m}$ and $x_2=5.1\mu\text{m}$. Left and right insets plot cross-sections along $x_0=3.3\mu\text{m}$ and $y_0=1.1\mu\text{m}$, respectively. From these cross-sections, we find that the trap frequency at the minimum along the x -axis is $\omega_x=1233\text{Hz}$, while along the y -axis it is $\omega_y=642\text{Hz}$. This corresponds to a ratio $\omega_x/\omega_y=1.92$, which confirms that it is possible to get a confining potential with similar curvatures in both transverse directions using this configuration. Notice that, with the same power, we could get other shapes for the BEC by changing the ratio ω_x/ω_y through the variation of H_w .

In conclusion, we have proposed a new class of optical BEC waveguides based on illuminating two waveguides built into a defect of a 1D-PhC. First, we have designed the structure to obtain a total atomic potential able to trap the condensate at $1\mu\text{m}$ from the surface. Secondly, we have optimized the potential in the plane perpendicular to the waveguides' axes to get a similar curvature at the minimum than that obtained in the direction normal to the surface. We have demonstrated that a power as low as 0.1mW is enough to guide a BEC of Cs atoms through the suggested waveguide. The kind of system proposed in this work could be considered as a basic ingredient for the development of novel BEC on-chip devices.

References:

1. E. Leanhardt *et al.*, Phys. Rev. Lett. **89**, 040401 (2002).
2. D.M. Stamper-Kurn *et al.*, Phys. Rev. Lett. **80**, 2027 (1998).
3. S. Inouye *et al.*, Nature **392**, 151 (1998).
4. M.J. Renn *et al.*, Phys. Rev. Lett. **75**, 3253 (1993).
5. H. Ito *et al.*, Phys. Rev. Lett. **76**, 4500 (1996).
6. J. Yin *et al.*, J. Opt. Soc. Am. B **15**, 25 (1998).
7. A.H. Barnett *et al.*, Phys. Rev. A **61**, 023608 (2000).
8. J. Arlt *et al.*, Phys. Rev. A **63**, 0630602 (2001).
9. J. P. Burke *et al.*, Phys. Rev. A **65**, 043411 (2004).
10. V.I. Balykin *et al.*, Phys. Rev. A **70**, 011401(R) (2004).
11. F.L. Kien, V.I. Balykin, and K. Hakuta, Phys. Rev. A **70**, 063403 (2004).
12. X. Luo *et al.*, Opt. Lett. **29**, 2145 (2004).
13. D. Rychtarik *et al.*, Phys. Rev. Lett. **92**, 173003 (2004).
14. R. Grimm, M. Weidemuller, and Y. Ovchinnikov, Adv. At. Mol. Opt. Phys. **42**, 95 (2000).
15. J.D. Joannopoulos, R.D. Meade, and J.N. Winn, *Photonic Crystals: Molding the Flow of Light* (Princeton University Press, Princeton, NJ, 1995).
16. H.A. Haus, *Waves and Fields in Optoelectronics* (Prentice-Hall, Englewood Cliffs, NJ, 1984).
17. S.G. Johnson and J.D. Joannopoulos, Opt. Express **8**, 173 (2001).
18. V.I. Balykin *et al.*, Rep. Prog. Phys. **63**, 1429 (2000).
19. Y.J. Lin *et al.*, Phys. Rev. Lett. **92**, 050404 (2004).
20. Z.C. Yan, A. Dalgarno, and J.F. Babb, Phys. Rev. A **55**, 2882 (1997).
21. Although the calculation of the Casimir-Polder attraction of the full multilayer structure would require a more detailed analysis, by assuming $\psi(\epsilon_{hi})$ we obtain an upper limit for the strength of this interaction.
22. A. Taflove and S.C. Hagness, *Computational Electrodynamics: the Finite-Difference Time-Domain Method*, 2nd ed. (Artech, Norwood, Mass., 2000).

Publications**Journal Articles Published**

- Rafif E. Hamam, Aristeidis Karalis, J. D. Joannopoulos, and Marin Soljacic. "Coupled-mode theory for general free-space resonant scattering of waves" Phys. Rev. A Vol.75, 053801, (2007).
- Evan J. Reed, Marin Soljacic, and J.D.Joannopoulos. "Maxwell equation simulations of coherent optical photon emission from shock waves in crystals" Phys. Rev. E Vol.75, 056611, (2007).
- Dye-Zone A. Chen, Rafif Hamam, Marin Soljacic, J.D.Joannopoulos, and Gang Chen. "Extraordinary optical transmission through subwavelength holes in a polaritonic silicon dioxide film" Appl. Phys. Lett. Vol.90, p.181921, (2007).
- D.L.C. Chan, I. Celanovic, J.D. Joannopoulos, JD, M. Soljačić, "Emulating one-dimensional resonant Q-matching behavior in a two-dimensional system via Fano resonances", Phys. Rev. A **74**, 064901 (2006).
- M. Bayindir, A.F. Abouraddy, O. Shapira, J. Viens, D. Saygin-Hinczewski, F. Sorin, J. Arnold, J.D. Joannopoulos, Y. Fink, "Kilometer-long ordered nanophotonic devices by preform-to-fiber fabrication", IEEE Journal of Selected Topics in Quantum Electronics **12**, 1202 (2006).

- J. Bravo-Abad, M. Ibanescu, J.D. Joannopoulos, M. Soljačić, "Photonic crystal optical waveguides for on-chip Bose-Einstein condensates", *Phys. Rev. A* **74**, 053619 (2006).
- B. Maes, M. Soljačić, J.D. Joannopoulos, P. Bienstman, R. Baets, S.P. Gorza, M. Haelterman, "Switching through symmetry breaking in coupled nonlinear micro-cavities", *Opt. Express* **14**, 10678 (2006).
- M. Soljačić, "Nanotechnology - New hope for optical signal processing", *Technology Review* **109**, 30 (2006).
- P. Bermel, A. Rodriguez, S.G. Johnson, J.D. Joannopoulos, M. Soljačić, "Single-photon all-optical switching using waveguide-cavity quantum electrodynamics", *Phys. Rev. A* **74**, 043818 (2006).
- A. Farjadpour, D. Roundy, A. Rodriguez, M. Ibanescu, P. Bermel, J.D. Joannopoulos, S.G. Johnson, G.W. Burr, "Improving accuracy by subpixel smoothing in the finite-difference time domain", *Opt. Lett.* **31**, 2972 (2006).
- D.L.C. Chan, M. Soljačić, J.D. Joannopoulos, "Direct calculation of thermal emission for three-dimensionally periodic photonic crystal slabs", *Phys. Rev. E* **74**, 036615 (2006).
- D.L.C. Chan, M. Soljačić, J.D. Joannopoulos, "Thermal emission and design in 2D-periodic metallic photonic crystal slabs", *Opt. Express* **14**, 8785 (2006).
- D.L.C. Chan, M. Soljačić, J.D. Joannopoulos, "Thermal emission and design in one-dimensional periodic metallic photonic crystal slabs", *Phys. Rev. E* **74**, 016609 (2006).
- A.F. Abouraddy, O. Shapira, M. Bayindir, J. Arnold, F. Sorin, D.S. Hinczewski, J.D. Joannopoulos, Y. Fink, "Large-scale optical-field measurements with geometric fibre constructs", *Nature Materials* **5**, 532 (2006).
- T.T. Ngo, C.M. Liddell, M. Ghebrebrhan, J.D. Joannopoulos, "Tetrastack: Colloidal diamond-inspired structure with omnidirectional photonic band gap for low refractive index contrast", *Appl. Phys. Lett.* **88**, 241920 (2006).
- O. Shapira, K. Kuriki, N.D. Orf, A.F. Abouraddy, G. Benoit, J.F. Viens, A. Rodriguez, M. Ibanescu, J.D. Joannopoulos, Y. Fink, M.M. Brewster, "Surface-emitting fiber lasers", *Opt. Express* **14**, 3929 (2006).
- P. Bermel, E. Lidorikis, Y. Fink, J.D. Joannopoulos, "Active materials embedded in photonic crystals and coupled to electromagnetic radiation", *Phys. Rev. B* **73**, 165125 (2006).
- M. Bayindir, A.E. Abouraddy, J. Arnold, J.D. Joannopoulos, Y. Fink, "Thermal-sensing fiber devices by multimaterial codrawing", *Advanced Materials* **18**, 845 (2006).
- E.J. Reed, M. Soljačić, J.D. Joannopoulos, Comment on "Explanation of the inverse doppler effect observed in nonlinear transmission lines", *Phys. Rev. Lett.* **96**, 069402 (2006).
- C.Y. Luo, M. Ibanescu, E.J. Reed, S.G. Johnson, J.D. Joannopoulos, "Doppler radiation emitted by an oscillating dipole moving inside a photonic band-gap crystal", *Phys. Rev. Lett.* **96**, 043903 (2006).
- E.J. Reed, M. Soljačić, J.D. Joannopoulos, Comment on "Explanation of the inverse doppler effect observed in nonlinear transmission lines", *Phys. Rev. Lett.* **96**, 069402 (2006).

- C.Y. Luo, M. Ibanescu, E.J. Reed, S.G. Johnson, J.D. Joannopoulos, "Doppler radiation emitted by an oscillating dipole moving inside a photonic band-gap crystal", *Phys. Rev. Lett.* **96**, 043903 (2006).
- P.T. Rakich, M.S. Dahlem, S. Tandon, M. Ibanescu, M. Soljačić, G.S. Petrich, J.D. Joannopoulos, L. A. Kolodziejski, E.P. Ippen, "Achieving centimetre-scale supercollimation in a large-area two-dimensional photonic crystal", *Nature Materials* **5**, 93 (2006).
- M. Ibanescu, E.J. Reed, J.D. Joannopoulos, "Enhanced photonic band-gap confinement via Van Hove saddle point singularities", *Phys. Rev. Lett.* **96**, 033904 (2006).
- E.J. Reed, M. Soljačić, R. Gee, J.D. Joannopoulos, "Coherent optical photons from shock waves in crystals", *Phys. Rev. Lett.* **96**, 013904 (2006).

